

Control of Surface Configuration of Nonuniformly Heated Shells

David Bushnell*

Lockheed Palo Alto Research Laboratories, Palo Alto, Calif.

The effectiveness of arbitrary distributions of concentrated loads (actuators) in controlling the surface quality of spherical caps and circular plates is determined by a numerical analysis. The residual root-mean-squared (rms) surface error of sandwich and monocoque shells is calculated as a function of the number, placement, and type of actuators. It is found that for a spherical cap with sandwich wall, diameter-to-thickness ratio of 400, and radius of curvature-to-thickness ratio of 2000, about 100 force actuators are required to reduce an initial rms surface error by two orders of magnitude.

Introduction

A BRIEF review of the literature on "active optics" is given in Ref. 1. By "active optics" is meant the control of one or more optical surfaces in an optical system to counteract the effects of changes in the environment. The results presented here are derived from the theory developed in Ref. 1. The main purpose of this paper is to determine rms residual errors in surfaces which have been warped by nonuniform temperature. This rms surface error is a function of the temperature distribution, the properties of the spherical cap, and the number, placement, and type of actuators.

The problem of counteracting initial surface distortions statically by means of application of various distributions of concentrated loads is treated with use of two computer programs, BOSOR6 and ACTUATOR. The BOSOR6 program² predicts the initial distortions of axisymmetric surfaces resulting from nonaxisymmetric temperature or other disturbance as well as the deflections caused by unit concentrated forces or unit self-equilibrating moment pairs which simulate force or moment actuators. Concentrated loads are expressed as Fourier series expansions of circumferentially varying line loads. In BOSOR6 the independent variables, meridional arc length s and circumferential coordinate θ , are separated. The meridional coordinate is discretized and the normal displacement distribution $f_n(s)$ for each Fourier harmonic is determined by minimization of a potential energy functional with respect to the nodal point displacement components. A collection of unit load influence functions $f_{in}(s)$, $i=1,2,\dots,I$; $n=0,1,2,\dots,N_{\max}$ is generated corresponding to actuators located at I different meridional (radial) stations and N_{\max} circumferential harmonics. The ACTUATOR program calculates actuator forces or moments that cause the mean-squared residual surface error to be minimized.

Numerical Results

Summary of Cases Analyzed

The method just described was used to investigate the behavior of various mirrors with diameter of 4 m. Table 1 gives the matrix of analyses performed. The radius of curvature of the shells is 20 m; each face sheet of the sandwich wall is 1-mm thick and the core is 8-mm thick; Young's modulus of the face sheets of the sandwich and of the monocoque shell is 6.74×10^{10} N/m² and of the core of the

sandwich is 6.74×10^3 N/m². Poisson's ratio is 0.3, and the thermal expansion coefficient is 0.03×10^{-6} per °C. In the thermal stress cases the temperature rise varies linearly through the thickness, being zero on the back face of the mirror. The mirror surface temperature is nonuniform along the meridian and around the circumference. In the BOSOR6 analysis 33 nodal points were used in the meridional discretization.

Distortions from Nonuniform Temperature Distribution

Figure 1 shows the temperature distribution and resulting initial distortion predicted by BOSOR6 for the 1-cm thick sandwich flat plate and the spherical cap. Four circumferential harmonics ($n=0,1,2,3$) are used for the nonuniform temperature distribution. The maximum temperature T_{\max} for each circumferential harmonic is arbitrarily chosen to be 1000°C, and the meridional variation of temperature for each of the harmonics $n=0,1,2$, and 3 is chosen in the form of a Zernike polynomial³ appropriate to that harmonic. The purpose of using Zernike polynomials is merely to cause mirror distortions of the sort that specialists in optics have names for, such as defocus ($n=0$), spherical aberration ($n=0$), tilt ($n=1$), coma ($n=1$), astigmatism ($n=2$), etc. The linear temperature gradient through the wall thickness gives rise to a rapidly varying normal displacement field near the edge of the mirror which requires many actuators to correct, as shall be seen.

Residual Surface Error as a Function of Number and Placement of Actuators

Figure 2 shows the initial distortions in the mirrors corresponding to the cases listed in Table 1 for force actuators, and the counteracting distortions caused by N actuators. The actuator loads are represented by Fourier cosine series with 40 harmonics. The residual surface error, not shown in Fig. 2, is the sum of the initial distortion and the counteracting distortion caused by the force actuators. The force actuators are represented as circumferentially varying line loads as given by Eq. (1) in Ref. 1. These line loads are spread over equal angle sectors ($-5 \text{ deg} \leq \theta \leq 5 \text{ deg}$), so that actuator forces at larger radii occur over longer arc lengths than do those at smaller radii, a physically unrealistic arrangement. However, as discussed in Ref. 1, the results obtained in this study are not sensitive to this local circumferential "smearing out" of the concentrated loads as long as the load is concentrated within a sector of less than about 10 deg. Figure 2A applies to the 1-cm thick sandwich shell. The initial distortion is caused by the nonuniform temperature field shown in Fig. 1a. Figure 2B applies to the 1-cm thick sandwich flat plate. The initial distortion is

Received March 27, 1978; revision received Aug. 24, 1978. Copyright © by David Bushnell. Published with permission by American Institute of Aeronautics and Astronautics, Inc.

Index category: Structural Design.

*Staff Scientist. Associate Fellow AIAA.

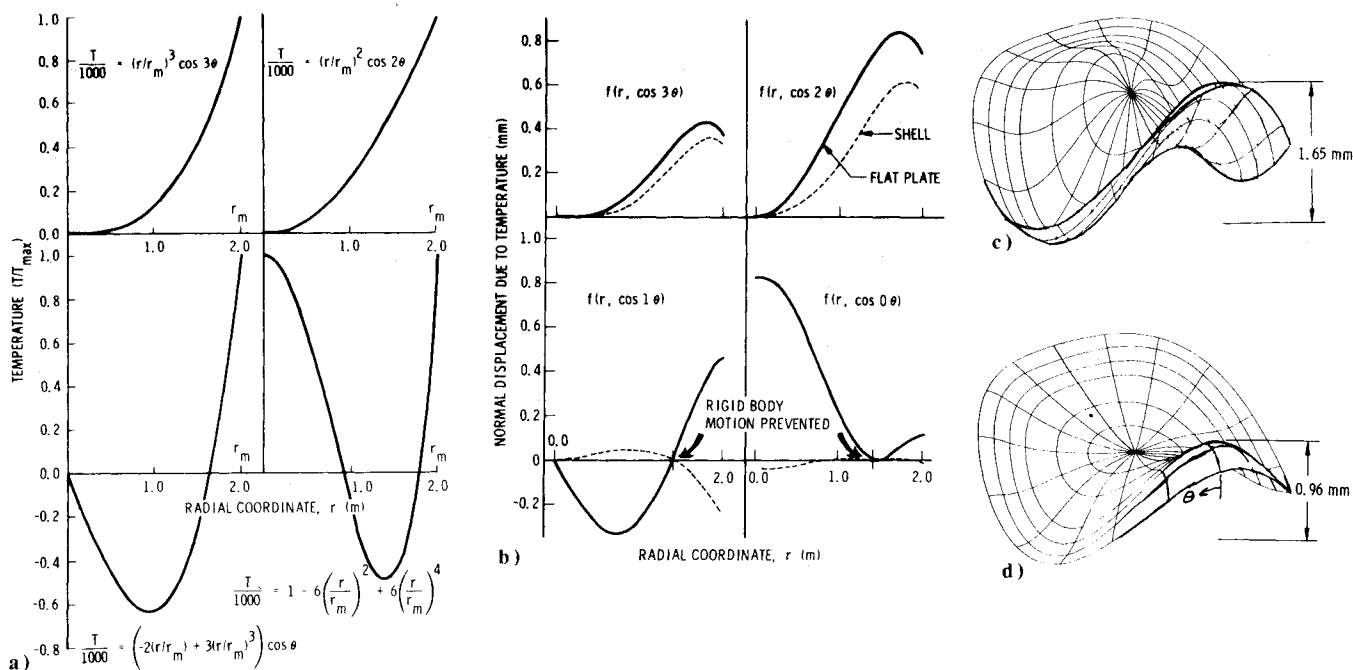


Fig. 1 Temperature rise on mirror surface and distortions generated in a sandwich flat plate and a spherical cap: a) meridional distribution of temperature rise at $\theta=0$ deg for four circumferential harmonics, $n=3, 2, 1$, and 0 , b) meridional distribution of normal displacement at $\theta=0$ deg for four circumferential harmonics, $n=3, 2, 1$, and 0 , c), d) isometric views of the distortion corresponding to a superposition of the four harmonic functions shown in b).

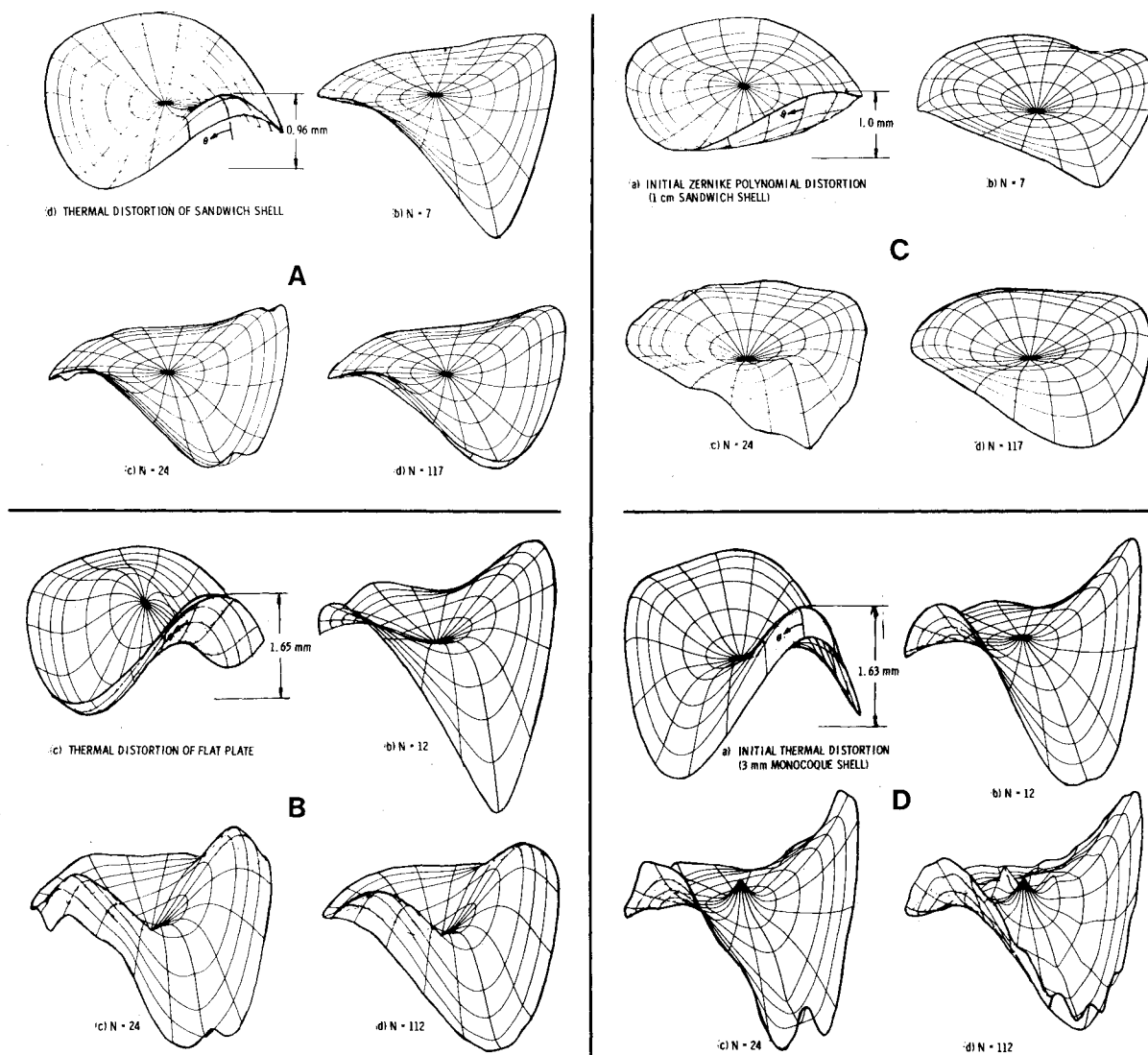


Fig. 2 Initial mirror distortions and counterdistortions caused by N force actuators trying to correct the initial distortion.

Table 1 Analysis matrix for the study of 4-m-diam curved and flat mirrors

Mirror geometry (diameter = 4 m)	Initial disturbance derived from thermal stress analysis	Distortion prescribed (Zernike polynomials)	Force actuators	Moment actuators
1-cm thick sandwich shell ($R = 20$ m)	X	X	X	X
1-cm thick sandwich flat plate	X		X	
3-mm thick monocoque shell ($R = 20$ m)	X		X	

generated as in Fig. 2A. Figure 2C applies to the 1-cm thick sandwich shell. The initial distortion is prescribed by Zernike polynomials with $n=0, 1, 2$, and 3 circumferential waves up to fourth order in r and even in θ . Figure 2D applies to the 3-mm thick monocoque shell. The initial distortion is generated by the nonuniform temperature field shown in Fig. 1a.

One of the most important parameters of this analysis is N_{\max} , the maximum number of circumferential waves used in the Fourier series representation of each concentrated actuator load. The residual rms surface configuration error ratio E [Eq. (11) of Ref. 1] is sensitive to N_{\max} if the number of actuators is fairly large and if an insufficient number of circumferential harmonics has been used to represent the actuator load. The initial distortions in the cases investigated here contain only harmonics less than or equal to $n=3$ circumferential waves. The low-order terms are approximately cancelled by the low-order terms of the Fourier series representation of the concentrated actuator loads, with the result that the residual surface error consists mainly of higher-order harmonics. Physically, these higher-order terms correspond to the local distortions generated by the actuators. Figure 3 clearly shows this effect. The ripples are most pronounced at the mirror edge near $\theta=0$ because of the relatively large actuator forces required there to counteract the localized bending generated by the thermal gradient through the mirror thickness. These actuator forces are shown in Fig. 8a. With a large number of actuators, it is necessary to use more than 20 circumferential harmonics for the series expansion for the line load [see Eq. (1) of Ref. 1] in order to obtain an accurate value of the rms error ratio E [$E = (\text{rms residual error})/(\text{rms initial error})$].

It is emphasized that in a two-dimensionally discretized finite-element model of this phenomenon it is necessary to use a much finer grid in order to obtain accurately the residual error E than would be required for accurate representation of the initial disturbance. Unfortunately, a too crudely discretized model leads to underestimation of the residual surface error.

As shown in Figs. 4a and 4b, the residual surface error ratio E is rather sensitive to the distribution of actuators, given a

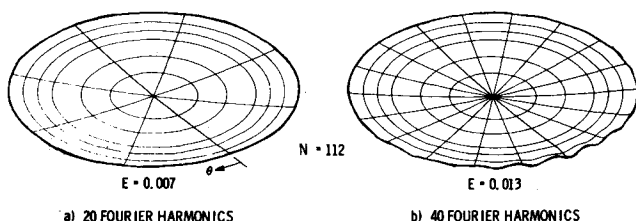


Fig. 3 Residual rms error in surface configuration for a nonuniformly heated 1-cm thick sandwich shell with $N=112$ force actuators.

constant number of them. The best distribution depends on the mirror properties and on the initial distortion to be corrected. Favorable actuator locations are determined from the results of numerical experiments. For the cases treated here it appears to be best to increase the actuator density somewhat toward the edge of the mirror and to stagger the circumferential locations at successive radii, as shown in the lowest right-hand case (No. 6) of Fig. 4a. It is not known at present whether this placement of actuators would be favorable for correction of most distortions likely to be encountered in practical applications.

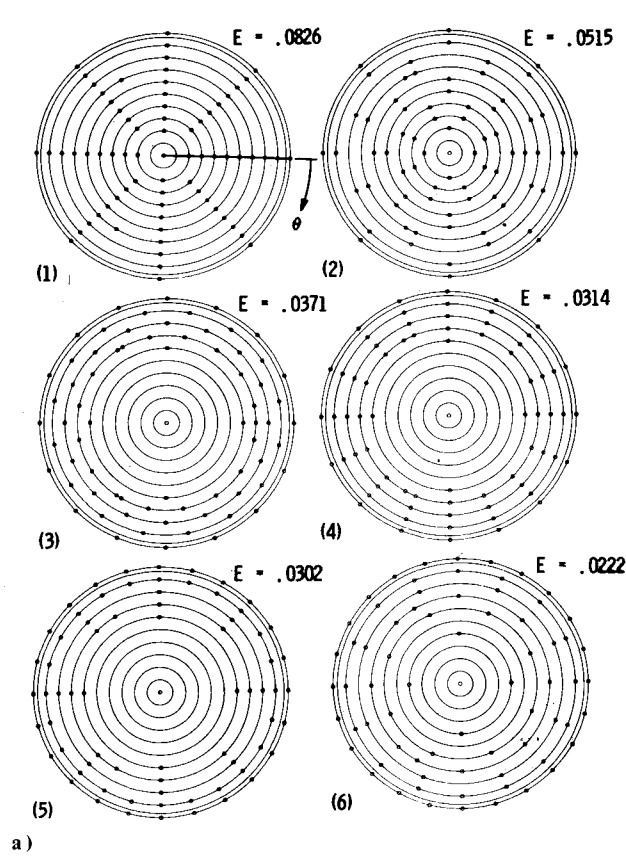
Figures 5-11 give the results of a study of the change in rms residual surface error with increasing numbers of actuators. Figure 5 shows the actuator distributions used in this investigation. Figure 6 gives the residual error vs the number of actuators for the 1-cm-thick sandwich shell with two different initial distortions, one generated by nonuniform temperature, as shown in Fig. 1d, and the other consisting of Zernike polynomials³ as follows:

$$w(r, \theta) = 0.2 \{ [1 + (2r^2 - 1) + (6r^4 - 6r^2 + 1)] + [r + (3r^3 - 2r)] \cos \theta + r^2 \cos 2\theta + r^3 \cos 3\theta \} \quad (1)$$

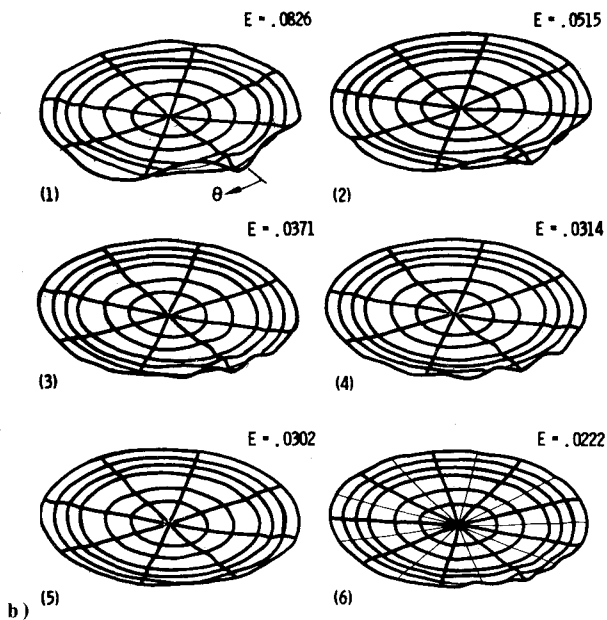
Figure 2C shows the initial Zernike polynomial distortions with certain $n=0$ and $n=1$ circumferential components removed for the best fit sphere, as shown in Fig. 5 of Ref. 1. For less than 20 actuators, the residual error for the thermally stressed mirror decreases much more rapidly than does the error for the Zernike distortion. Perhaps this is because the thermally induced distortions, arising as they do from a physical phenomenon, represent largely inextensional strains which can be approximately counteracted with few actuators. However, for more than 40 and less than about 100 actuators, the residual error for the thermally stressed mirror decreases more slowly than does the error for the Zernike distortion, probably because the temperature gradient through the mirror thickness give rise to local curling near $\theta=0$ which is difficult for the force actuators to counteract (see Fig. 1d).

Figure 7 demonstrates that effective correction cannot be achieved with a reasonable number of force actuators if the diameter-to-thickness ratio D/t and the radius of curvature-to-thickness ratio R/t are extremely high, as is the case for the 3-mm thick monocoque shell. The sandwich shell treated here acts much like a flat plate. The results for the flat plate, incidentally, are independent of D/t . In fact, given an initial temperature distribution, the residual errors shown here would hold approximately for mirrors with the same

$$\lambda = (D/t_e)^2 / (R/t_e) \quad (2)$$



a)



b)

Fig. 4 a) Actuator locations used for the study of the dependence of rms surface error ratio E on actuator distribution. The total number of actuators is held almost constant in this study ($N \approx 70$); b) rms error ratio E and residual surface error distribution for the thermally stressed 1-cm thick sandwich shell with force actuators distributed as shown in a.

In Eq. (2) t_e is the thickness of an equivalent monocoque wall, given by

$$t_e = \sqrt{3}t \quad (3)$$

where t is the total thickness of the sandwich wall.

Equation (3) is valid if the face sheets are thin compared to the total thickness t . For the flat plate $\lambda = 0$ and for the 1-cm thick sandwich shell $\lambda = 46.2$. The actuated mirror tested by

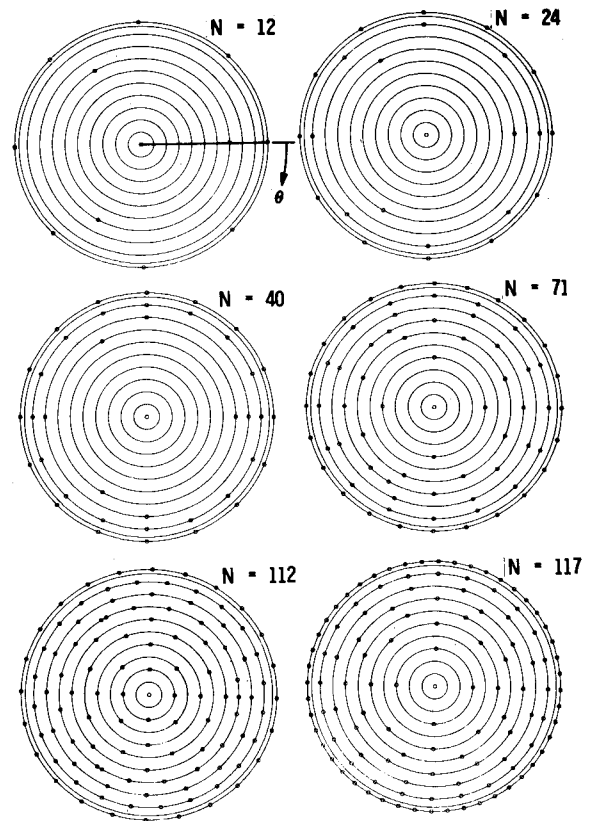


Fig. 5 Actuator locations used for the investigation of change in rms surface error ratio E with increasing number of actuators.

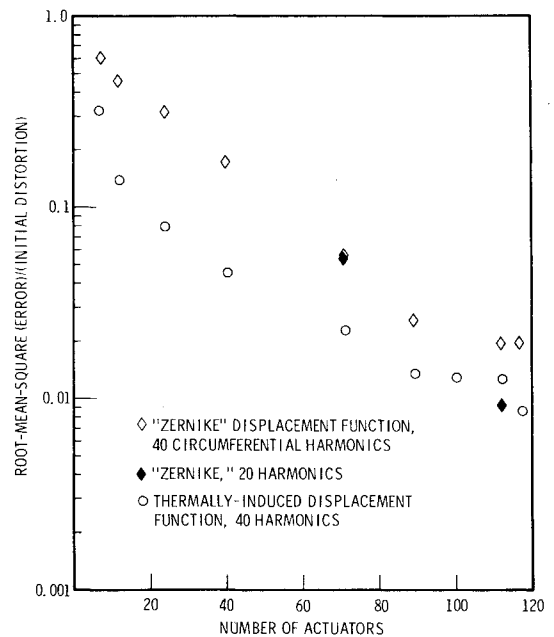


Fig. 6 rms surface error ratio E vs number of force actuators N for a 1-cm thick sandwich shell with two different initial distortions, that shown in Fig. 1d and that shown in Fig. 2C.

Robertson⁴ had $\lambda = 10.5$ and 60 actuators distributed uniformly over the surface. Notice that the point on the curve for the monocoque shell in Fig. 7 corresponding to the highest number of actuators ($N = 117$) is associated with a larger residual error than is the point for 112 actuators. In order to increase the number of actuators on the edge from 24 to 48, some actuators were removed from the interior region. Apparently this was a bad strategy for the very thin mirror. However, the same strategy was beneficial for the 1-cm thick

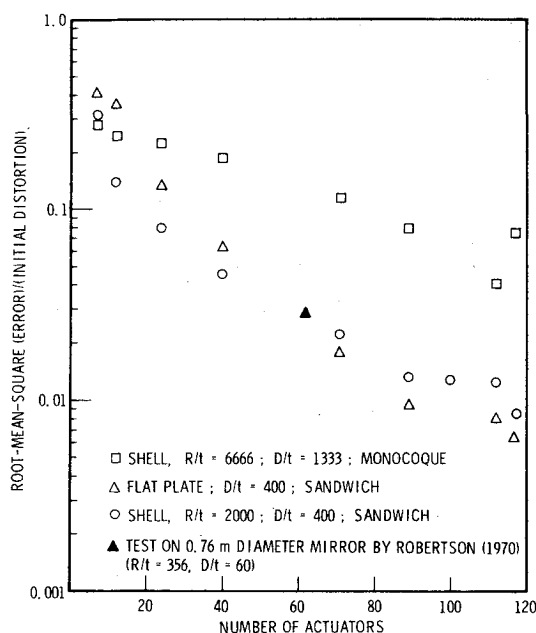


Fig. 7 rms surface error ratio E vs number of force actuators N for the three thermally stressed mirrors shown in Figs. 2A, B, and D.

sandwich shell and the flat plate. Thus, it is hard to tell intuitively what the most advantageous distribution of actuators is, even for known and fixed distortions. The present state-of-the-art is to determine the best actuator placement by numerical experiments. It would indeed be beneficial to have

some automated way of optimizing the actuator distribution given a fixed number of actuators.

From Fig. 7 it appears at first glance that the 1-cm thick sandwich flat plate will have a lower residual surface figure error than the 1-cm thick sandwich shell as long as there are more than about 60 actuators. However, the nonuniform temperature field given in Fig. 1a causes an initial rms distortion of 5.74×10^{-4} m in the flat plate but only 3.75×10^{-4} m in the shell. For $N = 117$ actuators the residual surface figure error is 3.71×10^{-6} m in the flat plate and 3.20×10^{-6} m in the shell. It turns out that for the particular temperature distribution and actuator distributions used in this analysis, the thin shell has the lowest residual error throughout the range of N investigated.

Figures 8 and 9 show the actuator force distributions and residual error for the four cases depicted in Fig. 2. The lengths of the arrows are proportional to the actuator forces. The largest residual errors are generally in the neighborhood of the edge of the mirror.

One can see from Fig. 10 that with more than about 80 actuators it is necessary to use more than 20 Fourier harmonics to represent the concentrated load. The point labeled "20 circumferential harmonics" for 112 actuators underestimates the residual error by approximately a factor of 2. This result indicates that a good design would have the actuators push against nonstructural pads that spread the concentrated loads over larger portions of the circumference without unduly increasing the actuator forces required to achieve a given correction.

Also shown in Fig. 10 is a curve of residual error vs number of self-equilibrating moment actuators of the type depicted in Fig. 11b. The slow rate of decrease of the surface configuration error with increasing number of moment actuators

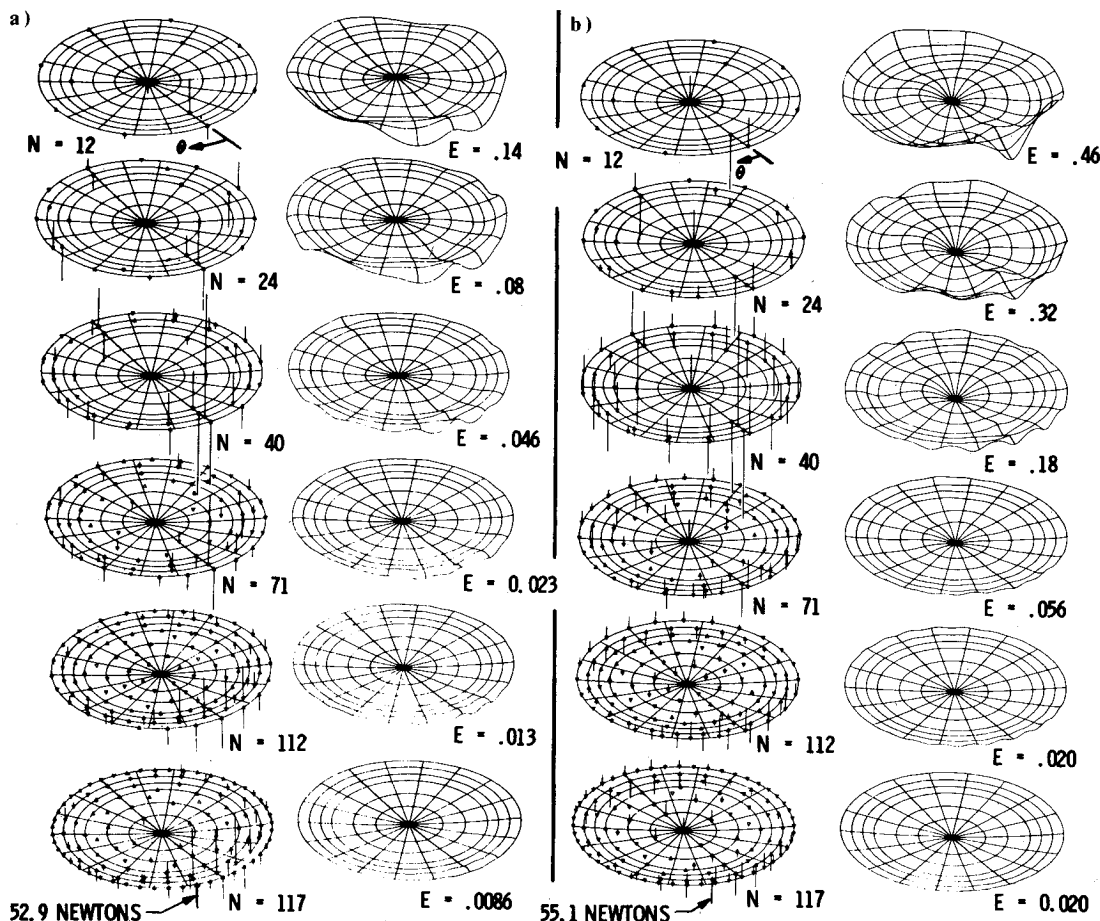


Fig. 8 Actuator forces and residual error for increasing number of actuators N . Actuators are distributed as shown in Fig. 5: a) 1-cm thick sandwich shell initially distorted by the nonuniform temperature distribution as shown in Fig. 1d, b) 1-cm thick sandwich shell initially distorted by prescribed Zernike polynomial normal displacements as shown in Fig. 2c.

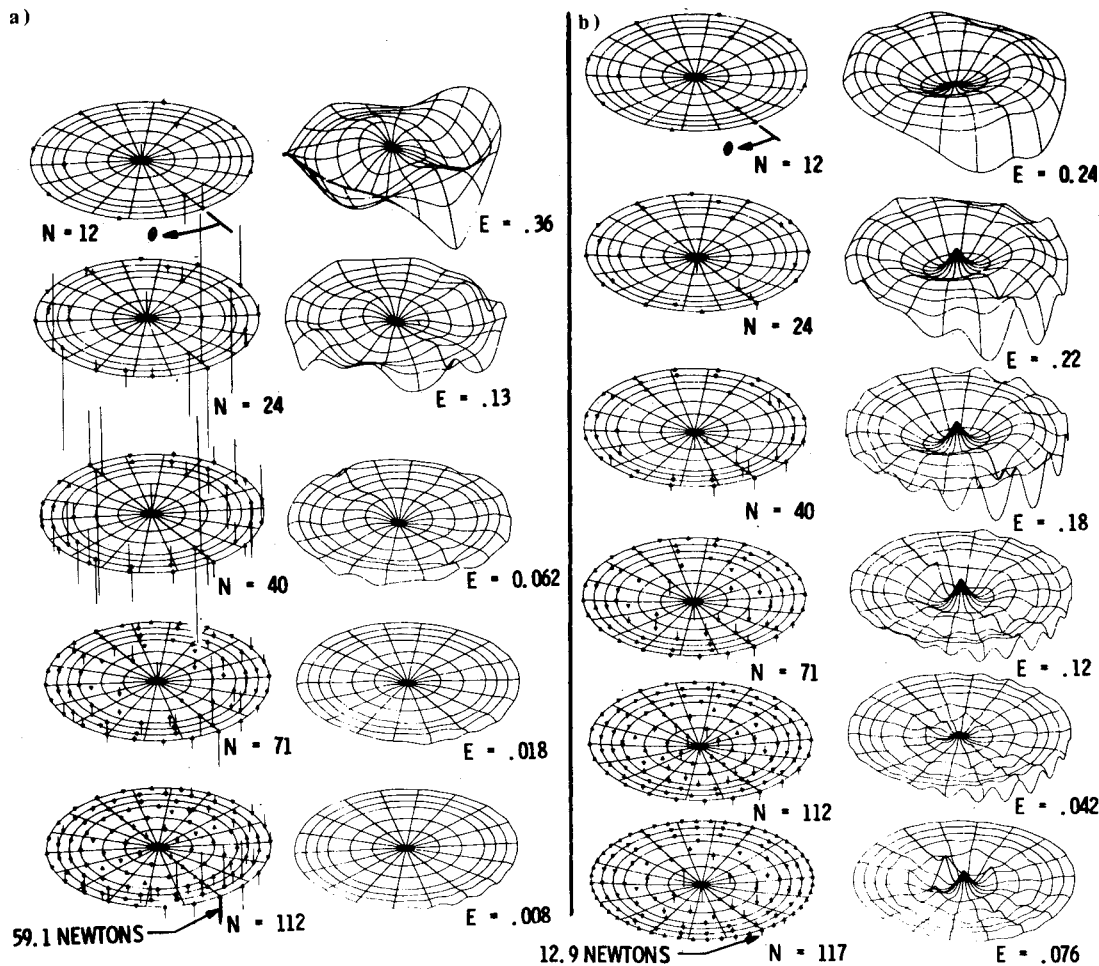


Fig. 9 Actuator forces and residual error for increasing number of actuators N . Actuators are distributed as shown in Fig. 5: a) 1-cm thick sandwich flat plate initially distorted by nonuniform temperature distribution as shown in Fig. 1c, b) 3-mm thick monocoque shell initially distorted by nonuniform temperature distribution as shown in Fig. 2D.

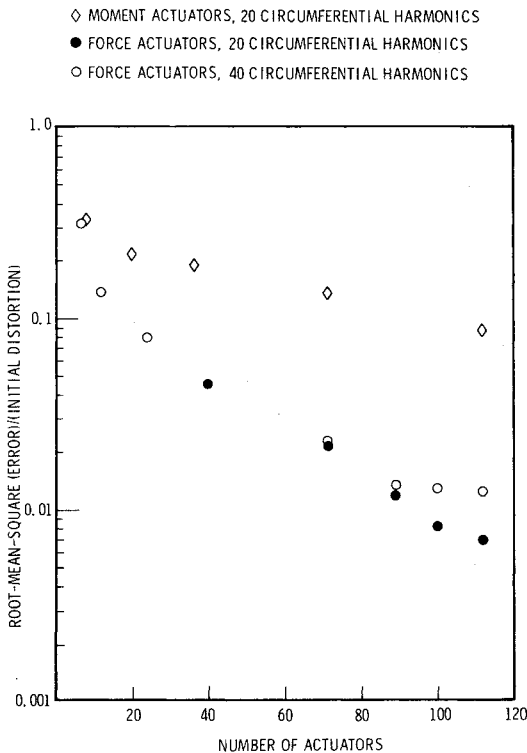


Fig. 10 rms surface error ratio E vs number of force or moment actuators for the 1-cm thick sandwich shell initially distorted by nonuniform temperature as shown in Fig. 1d.

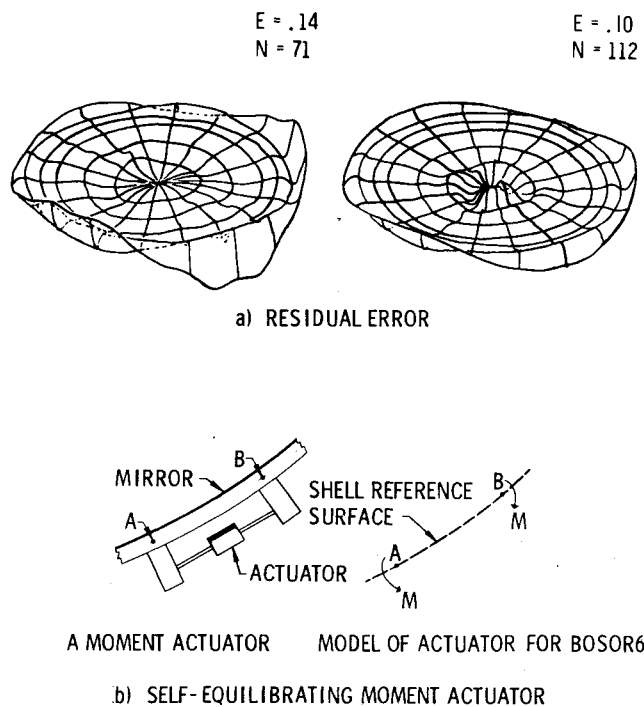


Fig. 11 rms error ratio E and residual surface figure error distribution for the 1-cm thick sandwich shell initially distorted by nonuniform temperature as shown in Fig. 1d and corrected by self-equilibrating moment actuators as distributed in Fig. 5. The arc length from A to B is 0.2 m.

is a result of the rather large amount of meridional waviness evident in Fig. 11 compared with that for similar distributions of force actuators as shown in Fig. 8a. The fact that there appear to be lower amplitude *circumferential* ripples in the case of moment actuation probably results from use of only 20 Fourier harmonics to represent the circumferential variation of each applied moment pair. Had 40 circumferential harmonics been used, the diamonds in Fig. 10 corresponding to more than 80 actuators would have been slightly higher. The difference would not have been so great as for the force actuation because the level of error due to *meridional* ripple is already quite high and would not have increased much. The conclusion from these calculations is that self-equilibrating moment actuators are not as efficient as force actuators for situations similar to that studied here.

Conclusions

In this paper, a continuation of Ref. 1, the rms residual surface figure error is calculated as a function of the number and distribution of actuators for sandwich and monocoque shells, a sandwich flat plate, force and self-equilibrating moment actuators, and two initial distortions, one resulting from nonuniform temperature and the other prescribed in the form of certain Zernike polynomials. It is found that as the number of actuators is increased, determination of the

residual error requires the use of an increasing number of circumferential harmonics in the Fourier series representation of the concentrated actuator forces or moments. Self-equilibrating moment actuators are not as effective as force actuators for the control of surface quality. Given a wall thickness, sandwich construction is better than monocoque because the higher ratio of bending stiffness to extensional stiffness of the sandwich leads to smaller residual errors with less pronounced local ripples. Of course, the sandwich shell is also less massive and the actuator forces required to counteract the initial error are smaller.

Acknowledgment

This work was sponsored by the Lockheed Missiles and Space Company 1977 Independent Research and Independent Development Programs.

References

- ¹Bushnell, D., "Control of Surface Shape by Application of Concentrated Loads," *AIAA Journal*, Vol. 17, Jan. 1979, pp. 71-77.
- ²Bushnell, D., "Stress, Buckling and Vibration of Hybrid Bodies of Revolution," *Computers and Structures*, Vol. 7, 1977, pp. 517-537.
- ³Born, M. and Wolf, E., *Principles of Optics*, 2nd ed., Pergamon Press, 1959, p. 465.
- ⁴Robertson, H. J., "Development of Active Optics Concept Using a Thin Deformable Mirror," NASA CR-1593, Aug. 1970.

From the AIAA Progress in Astronautics and Aeronautics Series...

EXPLORATION OF THE OUTER SOLAR SYSTEM—v. 50

Edited by Eugene W. Greenstadt, Murray Dryer, and Devrie S. Intriligator

During the past decade, propelled by the growing capability of the advanced nations of the world to rocket-launch space vehicles on precise interplanetary paths beyond Earth, strong scientific interest has developed in reaching the outer solar system in order to explore in detail many important physical features that simply cannot be determined by conventional astrophysical observation from Earth. The scientifically exciting exploration strategy for the outer solar system—planets beyond Mars, comets, and the interplanetary medium—has been outlined by NASA for the next decade that includes ten or more planet fly-bys, orbiters, and entry vehicles launched to reach Jupiter, Saturn, and Uranus; and still more launchings are in the initial planning stages.

This volume of the AIAA Progress in Astronautics and Aeronautics series offers a collection of original articles on the first results of such outer solar system exploration. It encompasses three distinct fields of inquiry: the major planets and satellites beyond Mars, comets entering the solar system, and the interplanetary medium containing mainly the particle emanations from the Sun.

Astrophysicists interested in outer solar system phenomena and astronautical engineers concerned with advanced scientific spacecraft will find the book worthy of study. It is recommended also as background to those who will participate in the planning of future solar system missions, particularly as the advent of the forthcoming Space Shuttle opens up new capabilities for such space explorations.

251 pp., 6x9, illus., \$15.00 Member \$24.00 List

TO ORDER WRITE: Publications Dept., AIAA, 1290 Avenue of the Americas, New York, N.Y. 10019